

Borexino's search for low-energy neutrinos associated with gravitational wave events from GWTC-3 database.

D. Basilico¹, G. Bellini¹, J. Benziger², R. Biondi^{a,3}, B. Caccianiga¹,
F. Calaprice⁴, A. Caminata⁵, A. Chepurinov⁶, D. D'Angelo¹, A. Derbin^{7,8},
A. Di Giacinto³, V. Di Marcello³, X.F. Ding^{b,4}, A. Di Ludovico^{c,4},
L. Di Noto⁵, I. Drachnev⁷, D. Franco⁹, C. Galbiati^{4,10}, C. Ghiano³,
M. Giammarchi¹, A. Goretti^{c,4}, M. Gromov^{6,11}, D. Guffanti^{d,12},
Aldo Ianni³, Andrea Ianni⁴, A. Jany¹³, V. Kobychev¹⁴, G. Korga^{15,16},
S. Kumaran^{e,17,18}, M. Laubenstein³, E. Litvinovich^{8,19}, P. Lombardi¹,
I. Lomskaya⁷, L. Ludhova^{17,18}, I. Machulin^{8,19}, J. Martyn¹², E. Meroni¹,
L. Miramonti¹, M. Misiaszek¹³, V. Muratova⁷, R. Nugmanov^{8,19},
L. Oberauer²⁰, V. Orekhov¹², F. Ortica²¹, M. Pallavicini⁵, L. Pelicci^{17,18},
Ö. Penek^{f,17}, L. Pietrofaccia^{c,4}, N. Pilipenko⁷, A. Pocar²², G. Raikov⁸,
M.T. Ranalli³, G. Ranucci¹, A. Razeto³, A. Re¹, N. Rossi³, S. Schönert²⁰,
D. Semenov⁷, G. Settanta^{g,17}, M. Skorokhvatov^{8,19}, A. Singhal^{17,18},
O. Smirnov¹¹, A. Sotnikov¹¹, R. Tartaglia³, G. Testera⁵, E. Unzhakov⁷,
A. Vishneva¹¹, R.B. Vogelaar²³, F. von Feilitzsch²⁰, M. Wojcik¹³,
M. Wurm¹², S. Zavatarelli⁵, K. Zuber²⁴, G. Zuzel¹³

¹Dipartimento di Fisica, Università degli Studi e INFN, 20133 Milano, Italy

²Chemical Engineering Department, Princeton University, Princeton, NJ 08544, USA

³INFN Laboratori Nazionali del Gran Sasso, 67010 Assergi (AQ), Italy

⁴Physics Department, Princeton University, Princeton, NJ 08544, USA

⁵Dipartimento di Fisica, Università degli Studi e INFN, 16146 Genova, Italy

⁶Lomonosov Moscow State University Skobel'syn Institute of Nuclear Physics, 119234 Moscow, Russia

⁷St. Petersburg Nuclear Physics Institute NRC Kurchatov Institute, 188350 Gatchina, Russia

⁸National Research Centre Kurchatov Institute, 123182 Moscow, Russia

⁹APC, Université de Paris, CNRS, Astroparticule et Cosmologie, Paris F-75013, France

¹⁰Gran Sasso Science Institute, 67100 L'Aquila, Italy

¹¹Joint Institute for Nuclear Research, 141980 Dubna, Russia

¹²Institute of Physics and Excellence Cluster PRISMA+, Johannes Gutenberg-Universität Mainz, 55099 Mainz, Germany

¹³M. Smoluchowski Institute of Physics, Jagiellonian University, 30348 Krakow, Poland

¹⁴Institute for Nuclear Research of NAS Ukraine, 03028 Kyiv, Ukraine

¹⁵Department of Physics, Royal Holloway, University of London, Egham, Surrey, TW20 OEX, UK

¹⁶Institute of Nuclear Research (Atomki), Debrecen, Hungary

¹⁷Institut für Kernphysik, Forschungszentrum Jülich, 52425 Jülich, Germany

¹⁸RWTH Aachen University, 52062 Aachen, Germany

¹⁹National Research Nuclear University MEPhI (Moscow Engineering Physics Institute), 115409 Moscow, Russia

²⁰Physik-Department, Technische Universität München, 85748 Garching, Germany

²¹Dipartimento di Chimica, Biologia e Biotecnologie, Università degli Studi e INFN, 06123 Perugia, Italy

²²Amherst Center for Fundamental Interactions and Physics Department, UMass, Amherst, MA 01003, USA

²³Physics Department, Virginia Polytechnic Institute and State University, Blacksburg, VA 24061, USA

²⁴Department of Physics, Technische Universität Dresden, 01062 Dresden, Germany

Received: date / Accepted: date

^aPresent address: Max-Planck-Institut für Kernphysik, 69117 Heidelberg, Germany

^bPresent address: IHEP Institute of High Energy Physics, 100049 Beijing, China

^cPresent address: INFN Laboratori Nazionali del Gran Sasso, 67010 Assergi (AQ), Italy

^dPresent address: Dipartimento di Fisica, Università degli Studi e INFN Milano-Bicocca, 20126 Milano, Italy

^ePresent address: Department of Physics and Astronomy, University of California, Irvine, California, USA

^fPresent address: GSI Helmholtzzentrum für Schwerionenforschung GmbH, 64291 Darmstadt, Germany

^gPresent address: Istituto Superiore per la Protezione e la Ricerca Ambientale, 00144 Roma, Italy

Abstract The search for neutrino events in correlation with gravitational wave (GW) events for three observing runs (O1, O2 and O3) from 09/2015 to 03/2020 has been performed using the Borexino data-set of the same period. We have searched for signals of neutrino-electron scattering with visible energies above 250 keV within a time window of ± 1000 s centered at the detection moment of a particular GW event. Two types of incoming neutrino spectra were considered: the mono-energetic line and the spectrum expected from supernovae. The same spectra were considered for electron antineutrinos detected through inverse beta-decay (IBD) reaction. GW candidates originated by merging binaries of black holes (BHBH), neutron stars (NSNS) and neutron star and black hole (NSBH) were analysed separately. In total, follow-ups of 74 out of 93 gravitational waves reported in the GWTC-3 catalog were analyzed and no statistically significant excess over the background was observed. As a result, the strongest upper limits on GW-associated neutrino and antineutrino fluences for all flavors (ν_e, ν_μ, ν_τ) have been obtained in the 0.5 – 5 MeV neutrino energy range.

Keywords Gravitational waves · neutrino · Borexino

1 Introduction

The era of multi-messenger astronomy has started with the detection of gravitational waves (GW) by the LIGO experiment [1]. During O1 and O2 observing periods (09/2015 – 08/2017), LIGO/Virgo has detected 10 binary black-hole mergers and a single binary neutron-star merger [2]. Firstly, the short gamma-ray burst GRB170817A was detected in 1.7 s temporal interval coincidence with the GW170817 event from the binary neutron-star merger [3]. At present the third LIGO, Virgo and KAGRA Collaboration Gravitational Wave Transient Catalog (GWTC-3) consists of transient GW signal records discovered up to the end of LIGO-Virgo’s third observing run (O3) [4].

The observation of GW events triggered an intensive follow-up campaign in neutrino detectors [5, 6, 7, 8, 9, 10, 11, 12, 13, 14, 15, 16, 17, 18, 19]. Čerenkov neutrino telescopes (ANTARES, IceCube [5, 10]) and Pierre Auger Observatory [6] have searched for high energy neutrinos above 100 GeV and 100 PeV, respectively. The experiment KamLAND has searched for inverse beta decay (IBD) antineutrino events within (1.8 – 111) MeV energy range [7, 16] and the Super-Kamiokande collaboration has reported results for neutrino signals within 3.5 MeV to 100 PeV energy range [8, 11, 17]. The Borexino detector has searched for correlated neutrino events with visible energies above 0.25 MeV within a

± 500 s time window centered at the detection moment of the first three reported GW events in assumption of monochromatic and Fermi-Dirac spectra [9]. The Daya Bay collaboration has searched for possible electron-antineutrino signals with energies from 1.8 to 100 MeV in coincidence with 7 GW events including GW 170817 within three time windows of ± 10 , ± 500 , and ± 1000 s relative to the occurrence of the GW events [13]. The XMASS-I 832 kg xenon detector has searched for event bursts associated with the 11 GW events detected during LIGO/Virgo’s O1 and O2 periods [15]. The NOvA neutrino detectors have performed search for any signal coincident with 28 GW events and supernova like neutrino interactions in coincidence with 76 GW events [12, 14]. The Baksan Underground Scintillation Telescope has searched for ν_μ and $\bar{\nu}_\mu$ with energies above 1 GeV from the directions of the localization of the GW events and in temporal coincidence with the GW170817 occurring due to the merger of two neutron stars [19, 18].

The neutrino and antineutrino events within a time window of ± 1000 (± 500 , ± 10) seconds around the moment of gravitational wave detection were analyzed in the detectors mentioned above, but no evidence for an excess of coincident neutrino events had been reported. Combination of the data from gravitational, neutrino and electromagnetic detectors forms a new multi-messenger approach leading to a deeper understanding of astrophysical and cosmological processes through combination of information from different probes.

Here, we report the results of a search for signals with visible energy above 0.25 MeV in the Borexino detector in coincidence with GW events from GWTC-3. We look for neutrino signals from $\nu_e, \nu_{x=\mu, \tau}$ and antineutrinos $\bar{\nu}_e, \bar{\nu}_{x=\mu, \tau}$ originated in the GW events that scatter on electrons. We also search for signals of $\bar{\nu}_e$ that induce IBD reaction on protons.

Two different spectra of incoming neutrinos ($\nu_{e,x}$ and $\bar{\nu}_{e,x}$) were used for the analysis: the mono-energetic line and the spectrum expected from supernovae. The same $\bar{\nu}_e$ -neutrino spectra were considered for search with the IBD reaction. The temporal correlation analysis between Borexino events and GW events were performed for three different merging modes of black holes and neutron stars - BHBH, NSNS, NSBH.

Negative results of searches for neutrino radiation accompanying GW events are presented as a limit on the neutrino or antineutrino fluences. In the papers above, the results of various detectors and different numbers of GW events were analyzed, sometimes the obtained limits of the neutrino fluence are normalized to the number of GW events. Since the data on the radiation mass M_{rad_i} and the distance to the event R_i

are available from the GWTC-3 catalog for almost all events, it would be natural, in assumption that the neutrino fluence has to be proportional to M_{rad_i} and inversely proportional to the square of R_i , to use this factor for comparison of the different experiments results.

2 The Borexino Detector

The Borexino is a liquid scintillator-based large volume detector specifically designed for neutrino detection. The experiment was located at the Laboratori Nazionali del Gran Sasso (LNGS) at the depth of 3800 meters of water equivalent and has been operated since from May 2007 till October 2021. Such location provided good cosmic muon flux suppression by a factor of $\approx 10^6$. The detector structure represents an implementation of the graded shielding concept.

The water tank (WT) is constructed of stainless steel with high radiopurity and contains 2100 tons of ultra-pure water as additional shielding imposed to suppress external γ -rays and neutrons. The WT contains a stainless steel sphere (SSS) with radius of 6.75 m and thickness of 8 mm that serves as the scintillating inner detector body. The WT is equipped with 208 8-inch PMTs placed on its floor and outer surface of the SSS and is used as the Cherenkov muon veto (outer detector, OD) for identification of residual muons crossing the detector. The scintillation light is detected by nominally 2212 8-inch PMTs of the inner detector (ID) uniformly distributed on the inner surface of the SSS. The neutrino target consists of 278 tons ultra-pure organic liquid scintillator and is confined in the innermost detector part, that is divided by two 125 μm nylon "balloons", the Radon Barrier (RB) and the Inner Vessel (IV) with radii of 5.50 m and 4.25 m respectively.

The scintillator was chosen for the purpose of low-energy neutrino registration as pseudocumene (PC 1,3,4-trimethylbenzene, $\text{C}_6\text{H}_3(\text{CH}_3)_3$) doped with a fluorescent constituent PPO (2,5-diphenyloxazole, $\text{C}_{15}\text{H}_{11}\text{NO}$) in concentration of 1.5 g/l. The buffer volume serves as neutron and gamma radiation shield and is posed with a solution of a light quencher dope consisting of 2 g/l dimethylphthalate (DMP, $\text{C}_6\text{H}_4(\text{COOCH}_3)_2$).

Detection of charged particles in the Borexino detector occurs via production of the scintillator light in the scintillator volume and its detection by the PMTs. Since the moment the detector started operation until the end of the experiment, the number of active PMTs has decreased that is taken into account in the current analysis. The data are used for reconstruction of energy and spatial coordinates of an event and also allow

to identify a particle type (e, α, μ) due to differences in the scintillation time profiles.

Both energy and spatial resolutions of the detector were studied with radioactive sources placed at different positions inside the inner vessel. The energy and position resolutions are $\sigma_E \approx 50$ keV and $\sigma_X \approx 10$ cm at 1 MeV with 2000 PMTs, respectively; both are scaling with the energy of an event as $\sim 1/\sqrt{E}$ at low energies. The primary electronics of the Borexino detector is optimized for energies up to few MeV with energy calibration reliable up to $E_{up} = 16.8$ MeV. For the purpose higher energies operation the system of 96 fast waveform 400 MHz digitizers was developed, each of them is reading-in the signal summed from 24 PMTs. The Borexino detector is unable to retain directional information of a single event due to nearly isotropic emission of scintillation light (see, however, [20,21]).

A more detailed description of the Borexino detector can be found in the following papers [22,23,24,25,26].

Neutrinos $\nu_{e,x}$ and antineutrinos and $\bar{\nu}_{e,x}$ are detected by means of their elastic scattering on electrons:

$$\nu_{e,x} (\bar{\nu}_{e,x}) + e^- \rightarrow \nu_{e,x} (\bar{\nu}_{e,x}) + e^- \quad (1)$$

For a given (anti)neutrino energy E_ν , the maximum electron recoil energy $E_{e_{max}}$ is given by the formula $E_{e_{max}} = 2E_\nu^2 / (2E_\nu + m_e)$ where m_e is the electron mass.

Electron antineutrinos $\bar{\nu}_e$ can also be detected via the inverse beta-decay (IBD) reaction with an energy threshold of 1.8 MeV:

$$\bar{\nu}_e + p \rightarrow n + e^+ \quad (2)$$

The visible energy of the positron and two annihilation photons is related to the antineutrino energy as $E_{vis} = E_{\bar{\nu}_e} - 0.784$ MeV. The neutron capture on protons produces a delayed 2.22 MeV γ 's with mean capture time of ~ 260 μs [27].

The Borexino was the first experiment that has detected and then precisely measured the ^7Be solar neutrino flux [28,29] as well as the ^8B -neutrino flux with 3 MeV threshold [30,31]. It has also observed pep -neutrinos for the first time [32], made the first spectral measurement of pp -neutrinos [33,34,26] and provided the first experimental evidence of solar neutrinos produced in the CNO cycle [35,36,37]. The Borexino detector has also registered antineutrinos $\bar{\nu}_e$ emitted in decay of radionuclides naturally occurring within the Earth [38,39,40,41].

Due to its excellent radiopurity, large target mass and low energy threshold, the Borexino detector is perfectly suited for the study of other fundamental problems, as well as searching for rare and exotic processes in particle physics and astrophysics.

The Borexino experiment has obtained new results on neutrino properties: ruled out any significant day-night asymmetry of the ${}^7\text{Be}$ neutrino interaction rate [42], it has set new limits on the effective magnetic moment of neutrinos [28], on the flux of $\bar{\nu}_e$ from the Sun [43, 44] and on the non-standard neutrino interactions [45]. A search for a number of rare low-energy processes has been carried out: possible violation of the Pauli exclusion principle [46], high-energy solar axions [47], heavy sterile neutrino mixing in the ${}^8\text{B}$ β^+ -decay [48], decay of an electron into a neutrino and a photon [49]. Additionally, temporal correlations with transient astrophysical sources such as γ -ray bursts [50], gravitational wave events [9], solar flares [44], and fast radio burst [51] have been performed.

3 The Borexino Data Selection

The aim of data selection is to provide maximum exposure for the desired study with minimum background contribution. In the current analysis we search for neutrino-electron scattering, a reaction that has no specific interaction signature. Thus, the background has to be suppressed generically, as a reduction of the detector count rate per unit of exposure. Background composition of the Borexino experiment was carefully studied in the course of many years of research. In the current study we account for the following background component groups:

- Short-lived cosmogenic backgrounds ($\tau \leq 1$ s) such as ${}^{12}\text{B}$, ${}^8\text{He}$, ${}^9\text{C}$, ${}^9\text{Li}$ etc., and long-lived cosmogenic backgrounds ($\tau \geq 1$ s) such as ${}^{11}\text{Be}$, ${}^{10}\text{C}$, ${}^{11}\text{C}$ etc., produced within the detector fiducial volume.
- External backgrounds present in the material of the inner nylon vessel such as ${}^{210}\text{Pb}$ and Uranium/Thorium decay chains.
- Internal natural backgrounds contained in the bulk of the detector fluid such as ${}^{14}\text{C}$, ${}^{85}\text{Kr}$, ${}^{210}\text{Bi}$ and ${}^{210}\text{Pb}$.

These backgrounds can be suppressed by using information coming from the processed detector data such as spatial event distributions or ID/OD temporal and spatial coincidences. Cosmogenic backgrounds are reduced by applying the detector temporal veto after each muon, which could be discriminated through coincidence with outer veto as well as by pulse-shape discrimination [27]. A veto duration of 0.3 s after each muon crossing the IV is applied to suppress ${}^{12}\text{B}$ to a statistically insignificant level and reduce ${}^8\text{He}$, ${}^9\text{C}$ and ${}^9\text{Li}$ by factor of 3 with a live time loss as small as 1 %. More long-lived cosmogenic backgrounds of ${}^{11}\text{C}$, ${}^{10}\text{C}$, ${}^{11}\text{Be}$ and others can was not specifically suppressed by

advanced veto system in order to save maximal exposure for neutrino events.

Backgrounds contained in the bulk of the detector can not be discriminated on event basis since they can not be localized neither spatially nor temporally. Nevertheless, the count rate of these background components are reduced by setting a cut on visible energy. This is important specifically due to the presence of ${}^{14}\text{C}$ in the scintillator. ${}^{14}\text{C}$ produces a beta-spectrum with an endpoint of 156 keV and has activity of roughly 110 Bq in the whole inner vessel.

The presence of this spectral component sets the lower threshold of the analysis to 0.25 MeV of visible energy¹. Two additional thresholds of 0.8 and 3 MeV of visible energy are applied for higher energy neutrino search. The second 0.8 MeV threshold was set in order to exclude ${}^{210}\text{Po}$ and solar ${}^7\text{Be}$ neutrino events and the third 3 MeV threshold rejects the most part of natural radioactivity.

Backgrounds contained in the nylon of IV can not be removed by any kind of purification and are therefore of the order of $10^2 - 10^3$ times higher than those within the bulk of the scintillator. The most important contributions come from ${}^{214}\text{Bi}$ and ${}^{208}\text{Tl}$ decays. These nuclides undergo β and $\beta + \gamma$ decay processes with a continuous spectrum overlapping with the region of interest of the current analysis. The most effective way to suppress this kind of backgrounds is to perform a geometrical cut on events, selecting those within a fiducial volume. The fiducial volume is defined in such manner that all events within and further than 75 cm away from the IV are kept. The distance of 75 cm corresponds to 3 standard deviations of position reconstruction uncertainty at the lowest 0.25 MeV energy threshold². The corresponding fiducial volume has a mass of 145 t.

4 GW events, temporal window and neutrino spectra

We have used the GWTC-3 database compiled by the LIGO and VIRGO collaborations for O1, O2 and O3 observing runs [4]. This database contains information about possible sources of GW events, merger time of the event in GPS seconds, mass M_1 and M_2 , chirp mass δM , final mass M_f in solar mass units, red-shift z , and distance information R .

During the period of interest from September 2015 to March 2020, 93 GW events have been observed, 87

¹Visible energy spectrum of ${}^{14}\text{C}$ is broadened up to this value due to energy resolution of the detector

²Position reconstruction precision increases with energy due to statistical reasons

of which are black hole mergers (BHBH), 2 events of neutron star merge (NSNS) and 4 events of neutron star - black hole merge (NSBH).

The nearest GW event is the most famous merger of two neutron stars GW170817 occurred at $R = 40_{-15}^{+7}$ Mpc. The biggest redshift $z = 1.18_{-0.53}^{+0.73}$ ($R = 8280_{-4290}^{+6720}$ Mpc) was observed for GW190403-051519. This was the only GW event with red shift $z > 1$, while 90% of the GW events have $z < 0.64$.

We have considered the coincidence time window $\Delta t = 2000$ s centered at the GW observation time with a width of ± 1000 s covering a possible delay of sub-MeV neutrinos propagating at the sublight speed. Negative interval of time window $\Delta t = 0.. -2000$ s covers earlier emission of neutrinos in the case of binary mergers [52]. For a distance corresponding to the $z = 0.64$ redshift, the delay will reach 1000 s in case of 0.6 MeV neutrinos with a rest mass of 65 meV, which is the upper limit on the heaviest neutrino mass state from the Planck 2018 data [53] and oscillation mass squared differences [54]. All selected GW events had the data taking time above 95% of the corresponding time interval Δt .

Since there is no reliable theory for the low-energy part of the neutrino emission spectrum for BHBH mergers, we calculated fluence limits for two different kinds of possible neutrino spectra: the monoenergetic line and the supernovae (SN) low-energy continuous spectrum $\Phi(E_\nu)$. The latter was assumed to be quasi-thermal spectrum with mean energy $\langle E \rangle$ and deviation from thermal distribution characterized by the pinching parameter $\alpha = 3$ for all neutrino flavors ($\nu_{e,x}, \bar{\nu}_{e,x}$) [55, 56, 57]. The emitted neutrino spectrum $S(E_\nu)$ depends on the neutrino energy E_ν as:

$$\Phi(E_\nu) \sim (E_\nu/T)^\alpha e^{(-E_\nu/T)}, \quad (3)$$

where $T = \langle E \rangle / (\alpha + 1)$ is effective temperature, which was considered to be the same for all neutrino flavors.

The expected number of events depends on neutrino spectrum and (ν, e) -scattering cross section $d\sigma(E_\nu)/dE_e$ [58]. The total cross section $\sigma(E_1, E_2)$ (e.g. $\sigma(E_{thr}, E_{e,max})$) for electron with energy in the range (E_1, E_2) is obtained by integrating the $d\sigma(E_\nu)/dE_e$ over recoil electron energies E_e between the electron energies E_1 and E_2 :

$$\sigma(E_1, E_2) = \int \frac{d\sigma(E_\nu, E_e)}{dE_e} dE_e \quad (4)$$

If the neutrino spectrum $\Phi(E_\nu)$ is not a monochromatic line, the total cross section for the electron recoil energy interval (E_1, E_2) is calculated as:

$$\sigma(E_1, E_2) = \int \int \frac{d\sigma(E_\nu, E_e)}{dE_e} \Phi(E_\nu) dE_e dE_\nu \quad (5)$$

Additionally, in order to compare the theoretical cross sections (4) and (5) with the experimental results, finite

energy resolution of the detector has to be taken into account [50]. The neutrino-electron cross sections, the number of electrons in the Borexino fiducial volume and the GW neutrino fluences will determine the expected number of neutrino events in the detector.

5 Analysis of the temporal correlations of Borexino signals with GW events

The Borexino detector was in data taking mode when 70 (out of 87) black hole mergers, 2 neutron star mergers and 2 (out of 4) neutron star black hole mergers have been occurred. Three different variants of binary merges in temporal coincidence with the Borexino data were analyzed separately. Some parameters of GW events involving neutron stars as obvious possible source of the neutrino flux are shown in Table 1. Additionally, average values of the these parameters for 70 BHBH mergers are shown in the bottom row of Table 1.

Table 1 GW events involving neutron stars, for which the temporal correlation analysis was carried out with the Borexino signals. $M1$ and $M2$ are masses in solar mass units M_\odot , R is distance in Mpc, M_{rad} is radiative mass in M_\odot units. Average values of $M1$, $M2$, R and M_{rad} are given for 70 black hole mergers.

GW event	Mode	$M1$	$M2$	R	M_{rad}
GW 170817	NSNS	1.46	1.27	40	≤ 0.04
GW 190425	NSNS	2.0	1.40	160	–
GW 190426	NSBH	5.7	1.5	370	–
GW 191219	NSBH	31.1	1.17	550	0.1
70 GW BHs	BHBH	36.7	23.0	2127	2.4

For the possible registration of neutrinos, the most interesting is the GW170817 signal measured on 2017 August 17 produced by the coalescence of two neutron stars with masses $1.46 M_\odot$ and $1.27 M_\odot$ and occurred at a record close distance $R = 40_{-15}^{+7}$ Mpc. The second registered neutron star merger GW190425 event occurred at a distance 4 times greater with the close chirp mass, which determines the amplitude of the GW signal.

The detection time and energy of Borexino events passing all data selection cuts in ± 5000 s windows around GW170817 and GW190425 events due to the merger of two neutron stars are shown in Figure 1. The closest events with energies 1.54 (2.41) MeV occurred at 610 (154) s before GW170817 (GW190425), respectively. A similar Figure 2 shows Borexino events for two GW190426 and GW191219 events corresponding to the merger of a neutron star and a black hole.

Number of Borexino events in ± 1000 s interval with energy above 0.25 MeV (N_1) and 0.8 MeV (N_2) in

comparison with the reduced backgrounds defined for intervals $[-5000 \dots -1000, 1000 \dots 5000]$ s are shown in Table 2 for 4 GW events involving neutron stars. One can see that no excess of the counting rate, associated with GW events involving neutron stars, above the expected background is observed. So, there are only 3 events in the ± 1000 s interval centered at the GW170817 event arrival time with the energy in the 0.25 – 16.8 MeV range, while 2.5 ± 0.8 solar neutrino and background reduced events were obtained within the $[-5000 \dots -1000, 1000 \dots 5000]$ s window. All detected events were in agreement with expected solar neutrino and background count rates.

As noted above, the Borexino detector was in data taking mode when 70 black hole mergers have been occurred. The energy spectrum of Borexino events in correlation with BHBH GW events in the ± 1000 s time window for 150 keV interval and the normalized background spectrum of events registered in $[-5000 \dots -1000]$ s and $[1000 \dots 5000]$ s intervals are shown in Figure 3.

Number of events and the reduced background in ± 1000 s interval with energy above 0.25 MeV and 0.8 MeV for 70 GW BHBH events are shown in Table 2. No statistically significant excess of the difference between these spectra for any energy interval was observed.

The spectrum in Figure 3 is dominated by ^{14}C in the region below 0.250 MeV of visible energy, by the recoil electrons from solar ^7Be neutrinos in 0.25 – 0.8 MeV interval, by cosmogenic ^{11}C in 1 – 2 MeV region and by external gamma-quanta of ^{214}Bi and ^{208}Tl in 2 – 3 MeV region. All these components can not be significantly reduced by any available data selection techniques without serious exposure loss. Figure 3 shows the energy spectrum in the range 0.25-4.0 MeV and only three events were detected with energies above 4 MeV.

Table 2 Number of events N_1 and N_2 in ± 1000 s interval with energies above 0.25 MeV and 0.8 MeV, correspondingly, for GW events involving neutron stars. For comparison the reduced backgrounds B_1 and B_2 defined for intervals $[-5000 \dots -1000, 1000 \dots 5000]$ s are also shown. The same data for 70 BHBH GW events is shown in the last column.

GW	170817	190425	190426	191219	70 GWs
mode	NSNS	NSNS	NSBH	NSBH	BHBH
N_1	3	4	2	9	304
B_1	2.5 ± 0.8	4.3 ± 1.0	4.8 ± 1.1	4.3 ± 1.1	310 ± 9
N_2	3	2	1	4	158
B_2	1.8 ± 0.7	2.0 ± 0.7	2.8 ± 0.8	3.0 ± 0.9	163 ± 7

Based on the spectrum of the Borexino detector in Figure 3 three mentioned above energy thresholds are

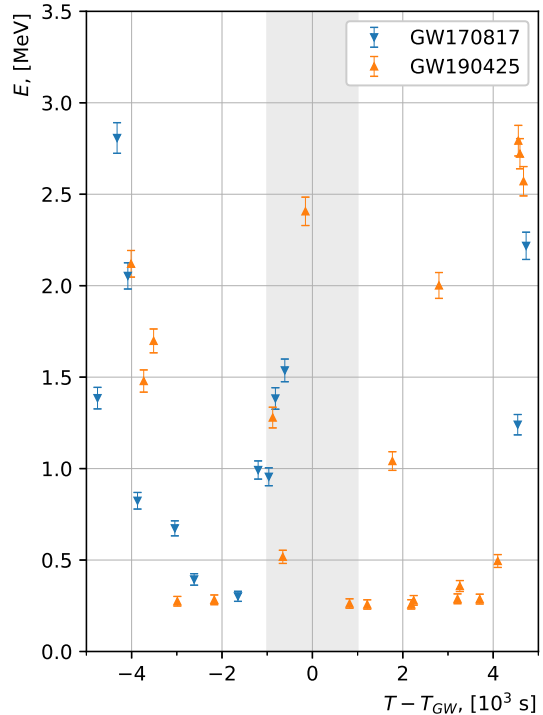


Fig. 1 Borexino events with energies above 0.25 MeV occurring within ± 5000 s of GW170817 (blue inverted triangles) and GW190425 (yellow triangles) events produced by the coalescence of two neutron stars. All events are consistent with the expected rates of solar neutrinos and background events.

selected for the analysis: $E_1 = 0.25$ MeV, $E_2 = 0.8$ MeV and $E_3 = 3.0$ MeV. The analysis is performed for the energy intervals from $E_{1,2,3}$ to $E_{e_{max}}$, the latter must not exceed the range of validity of the detector energy response calibration E_{up} . In the analysis, the energy resolution of the detector $\sigma(E_e)$ is taken into account [50]. The threshold of 0.25 MeV allows to register neutrinos with energy as low as 0.4 MeV via neutrino–electron elastic scattering.

The analysis consisted in search for an excess of selected events above the measured background, in coincidence with GW events in a time window of $\Delta t = 2000$ s centered at the GW event arrival times. We calculated the overall number of candidate events above 0.25 MeV, 0.8 MeV and 3.0 MeV in the Δt interval for various values of neutrino energy E_ν or average energy $\langle E \rangle$ for SN spectra, which met the requirements for selection cuts of the described data.

Since there is no statistically significant excess of the number of events within ± 1000 s GW window above the background, the upper limits on fluences $\Phi_{\nu_{e,x}, \bar{\nu}_{e,x}}$ for

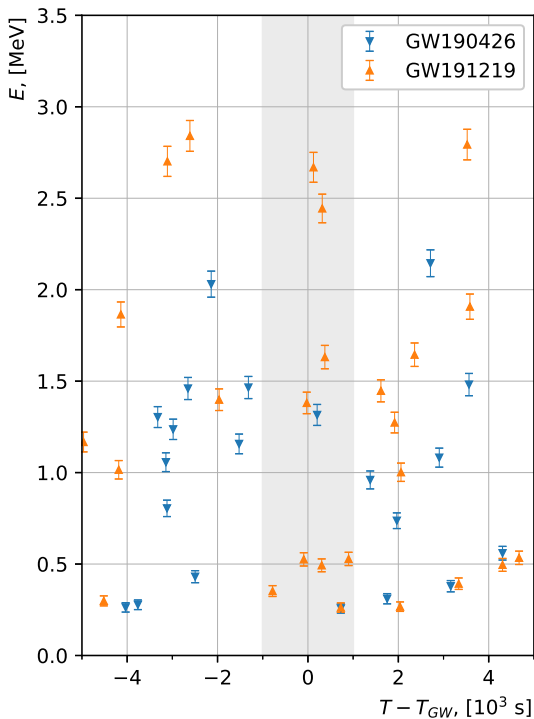


Fig. 2 Borexino events with energies above 0.25 MeV occurring within ± 5000 s of GW190426 (blue inverted triangles) and GW191219 (yellow triangles) events produced by the coalescence of neutron star and black hole.

mono-energetic (anti)neutrinos with the energy E_ν are calculated as:

$$\Phi_{\nu_{e,x}, \bar{\nu}_{e,x}} = \frac{N_{90}(E_\nu, n_{obs}, n_{bkg})}{r N_e \sigma(E_{th}, E_{e_{max}})}, \quad (6)$$

where $N_{90}(E_\nu, n_{obs}, n_{bkg})$ is the 90% C.L. upper limit for the number of GW-correlated events in the $(E_{th}, E_{e_{max}})$ interval per single GW and N_e is the number of electrons in 145 t of the Borexino scintillator. The limits were obtained in assumption that the whole neutrino fluence consists of only one individual flavor. The factor $\sigma(E_{th}, E_{e_{max}})$ represents the cross section for detected neutrinos ($\nu_{e,x}, \bar{\nu}_{e,x}$) with the energy E_ν without oscillations while recoil electrons are detected in the interval $(E_{th}, E_{e_{max}})$ taking into account the detector energy resolution [50]. The recoil electron detection efficiency r was taken as 1, with the accuracy corresponding to the precision of the fiducial volume definition ($\simeq 1\%$ [34]).

The numerator $N_{90}(E_\nu, n_{obs}, n_{bkg})$ was calculated with correlated and uncorrelated GW spectra in the energy interval $(E_{th}, E_{e_{max}})$. Here, n_{obs} and n_{bkg} denote overall numbers of observed and background events in this energy interval normalized by their respective times. The longer interval $\Delta t_{bkg} = 18$ ks for background detection was chosen in order to reduce the error of n_{bkg}

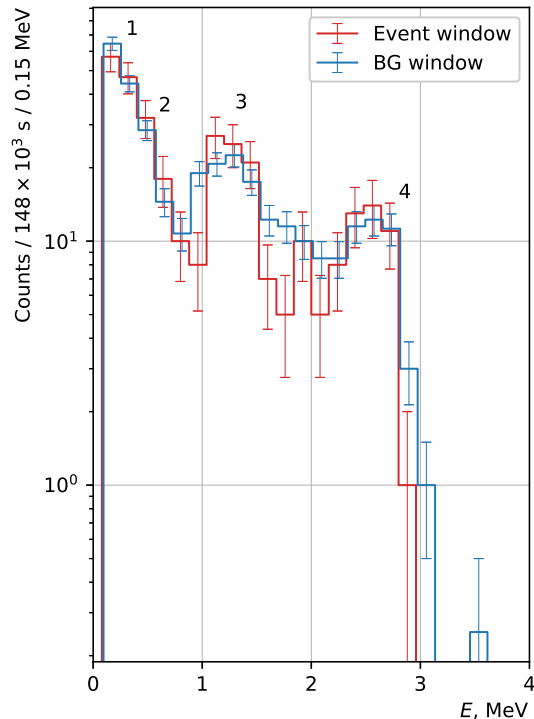


Fig. 3 Borexino visible energy spectrum of singles in correlation with 70 BHBH GW events in the ± 1000 s time window (red line with errors). Blue line shows the normalized background spectrum measured in $[-5000 \dots -1000]$ s and $[1000 \dots 5000]$ s intervals. 1 - ^{210}Po α -peak, 2 - recoiled electrons from the solar ^7Be -neutrino, 3 - ^{11}C β^+ -decay, 4 - external background (^{208}Tl).

that plays an important role in the Feldman-Cousins method. The value n_{bkg} was normalized by the overall time ratio taking into account the actual live time of the detector within these time windows.

The procedure was repeated for neutrino energies E_ν from 0.5 MeV to 50 MeV in increments of 0.5 MeV. The region of neutrino energies up to 50 MeV was chosen in accordance with the characteristic energies of neutrinos appearing in the pion decay at rest. As was mentioned above, in order to have the best ratio of the expected effect with respect to the background and taking into account the shape of the spectrum (Figure 3) the three energy thresholds E_1 , E_2 and E_3 were used for different neutrino energies. The analysis is performed in the energy interval $(E_{1,2,3}, E_{e_{max}})$ if $E_{e_{max}}$ is not exceeded E_{up} , in the later case the value E_{up} was used for the right border of the analysis interval.

For the case of all 74 GW events the upper limits on neutrino and antineutrino fluences of different flavors normalized per single GW are shown in Figure 4. The jumps in the upper limit at the energies above 7 MeV is associated with the inclusion of the

above-mentioned three events with energies above 4 MeV in the analysis. The limits reach a constant level at higher neutrino energies above 17 MeV due to the fact that the maximum energy of recoil electrons $E_{e,max}$ is constrained by the value $E_{up} = 16.8$ MeV in the analysis. These are the first constraints on the fluence of neutrino with energy below 4 MeV obtained from the neutrino-electron scattering reaction. The previous limits obtained by Super-Kamiokande collaboration for the GW170817 NSNS merger with $(\nu_{e,x}, e)$ - and $(\bar{\nu}_x, e)$ -scattering are also shown in the Figure 4 [11].

Since there is no reliable model for the low-energy neutrino spectrum of GW events, we perform calculations of neutrino emission from a supernova collapse [55,56,57]. Assuming quasi-thermal distributions (3) with a mean energy $\langle E \rangle = 15.6$ MeV and the parameter $\alpha = 3$ and integrating over the analyzed electron recoil energy interval $E_{1,2,3} - E_{up}$ MeV, we get the limits on the total electron neutrino fluence per single GW: $\Phi(\nu_e) \leq 1.2 \times 10^{10} \text{cm}^{-2}$ (90% C.L.) that is close to the limit obtained for mono-energetic neutrinos with the same energy. The values of the limits on other neutrino flavors obtained from the (ν, e) -scattering channel are given in Table 3. We also calculated the upper limit on the electron antineutrinos ($\bar{\nu}_e$) fluence given in Table 3 using the IBD reaction (see section 8).

Table 3 Upper limits on fluences from all 74 events per single GW for all neutrino flavors obtained from the temporal correlation analysis in 10^9cm^{-2} units (90% C.L.) calculated for mono-energetic neutrinos and the SN spectrum with $\langle E \rangle = 15.6$ MeV.

E_ν	Φ_{ν_e}	$\Phi_{\bar{\nu}_e}$	$\Phi_{\nu_{\mu,\tau}}$	$\Phi_{\bar{\nu}_{\mu,\tau}}$	IBD
2	654	1805	3434	4108	104
6	35.3	200	220	287	1.70
10	17.8	67.9	110	139	0.51
14	16.0	52.3	97.4	121	0.25
18	12.3	35.7	74.2	91.1	—
30	12.0	21.9	65.6	75.3	—
50	11.8	16.6	59.8	65.7	—
$< 15.6 >$	12.2	18.5	63.3	70.6	—

6 Limits on neutrino fluences from GW events involving neutron stars

The limits on $\nu_{e,x}$ and $\bar{\nu}_{e,x}$ fluence were alternatively obtained for NSNS and NSBH GW events. The intervals for the analysis ($E_{1,2,3}, E_{e,max}$) are set to the same way as previously described. The values of the monoenergetic neutrino energy E_ν and the supernova neutrino mean energy $\langle E \rangle$ from 0.5 to 50 MeV in increments of 0.5 MeV, the expected spectra of recoil elec-

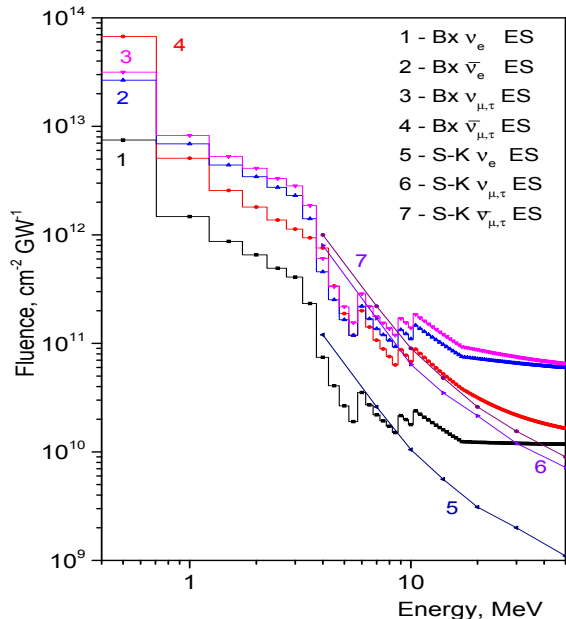


Fig. 4 Upper limits on mono-energetic neutrino fluences obtained with (ν, e) elastic scattering reaction (ES) through the temporal correlation analysis for 74 GW events (90% C.L.): 1 - ν_e , 2 - $\nu_{\mu,\tau}$, 3 - $\bar{\nu}_e$, 4 - $\bar{\nu}_{\mu,\tau}$. The limits 5, 6 and 7 of Super-Kamiokande obtained for single GW170817 event from (ν, e) -scattering reaction are also shown [11].

trons and the number of detected events in the interval ($E_{1,2,3}, E_{e,max}$) were used in the calculations.

The relation (6) was converted into the obtained fluence limits for all neutrino flavors given in Figure 5 for NSNS GW 170817 event and in Figure 6 for NSBH GW 190426 and GW 191219 events, both for mono-energetic neutrinos and for supernova neutrinos. We only analyzed the first NSNS GW 170817 event separately, since the second NSNS GW 190425 event occurred at a distance 4 times further, and the exactly GW 170817 event was analyzed by almost all of the above-mentioned neutrino detectors.

At neutrino energies above 17 MeV, the limits become almost constant since the (ν, e) -scattering cross section is proportional to E_ν and the spectrum of recoil electrons weakly depends on the electron energy.

The results for the NSNS case are also shown in Table 4 for mono-energetic neutrinos. In case of the supernova neutrino spectrum, the fluence constraints are slightly stronger than the monoenergetic neutrino limit at $\langle E \rangle = E_\nu$ (Table 5).

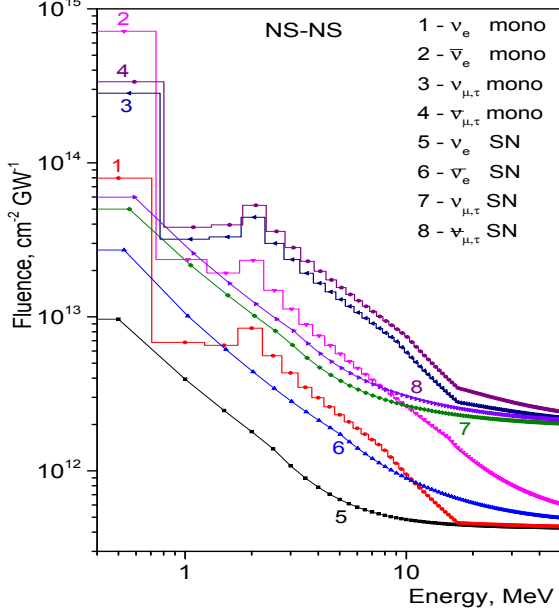


Fig. 5 The merger of two neutron stars - GW170817 event. The upper limits on the fluences of monoenergetic neutrinos - $1-\nu_e$, $2-\bar{\nu}_e$, $3-\nu_{\mu,\tau}$, $4-\bar{\nu}_{\mu,\tau}$ and neutrinos with SN spectra - $5-\nu_e$, $6-\bar{\nu}_e$, $7-\nu_{\mu,\tau}$, $8-\bar{\nu}_{\mu,\tau}$ (90% C.L.). The x-scale shows the energy of monoenergetic neutrinos E_ν or the average energy $\langle E \rangle$ in the case of a supernova spectrum.

Table 4 Borexino 90% C.L. upper limits for the fluences of all neutrino flavours from NSNS GW 170817 event, obtained through the study of (ν, e) elastic scattering of monoenergetic neutrinos and IBD reaction. E_ν is given in MeV units, $\Phi_{\nu_{e,x}, \bar{\nu}_{e,x}}$ - in 10^{12} cm^{-2} units.

E_ν	Φ_{ν_e}	$\Phi_{\bar{\nu}_e}$	$\Phi_{\nu_{\mu,\tau}}$	$\Phi_{\bar{\nu}_{\mu,\tau}}$	IBD
2	8.44	23.3	44.3	53.0	3.80
6	1.89	4.65	10.7	12.7	0.0622
10	0.950	2.62	5.85	7.41	0.0186
14	0.593	1.83	3.61	4.50	0.0090
18	0.458	1.32	2.75	3.38	0.0054
30	0.444	0.810	2.43	2.79	—
50	0.435	0.613	2.22	2.43	—

7 Limits on the neutrino fluences from the selected most intensive BHBH GW events.

Since for almost all GW events the distance to the event R_i and the radiation mass M_{rad_i} are known (with some accuracy), in contrast to gamma-ray bursts or fast radio bursts cases [50, 51], it is possible to obtain the limit on the neutrino fluence for some hypothetical standard event at a fixed distance and with a known radiative mass. This allows to compare the obtained limits on the neutrino fluence for a different set of GW events. The

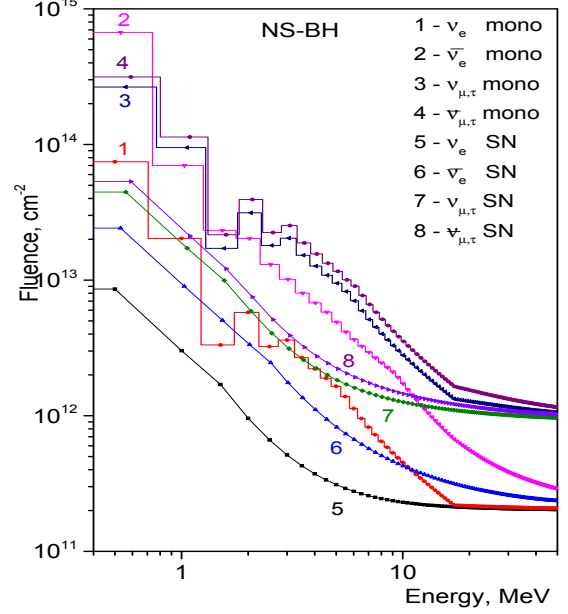


Fig. 6 The merger of neutron star and black hole - GW190426 and GW191219 events. The upper limits on the fluences of monoenergetic neutrinos (Energy = E_ν) - $1-\nu_e$, $2-\bar{\nu}_e$, $3-\nu_{\mu,\tau}$, $4-\bar{\nu}_{\mu,\tau}$ and neutrinos with SN spectra (Energy= $\langle E \rangle$) - $5-\nu_e$, $6-\bar{\nu}_e$, $7-\nu_{\mu,\tau}$, $8-\bar{\nu}_{\mu,\tau}$ (90% C.L.).

Table 5 Borexino 90% C.L. upper limits for the fluences of all neutrino flavours from NSNS GW 170817 event, obtained through the study of (ν, e) elastic scattering of neutrino with supernova spectrum and IBD reaction. $\langle E \rangle$ is given in MeV units, $\Phi_{\nu_{e,x}, \bar{\nu}_{e,x}}$ - in 10^{12} cm^{-2} units.

$\langle E \rangle$	Φ_{ν_e}	$\Phi_{\bar{\nu}_e}$	$\Phi_{\nu_{\mu,\tau}}$	$\Phi_{\bar{\nu}_{\mu,\tau}}$	IBD
2	1.80	4.39	10.2	12.1	1.67
6	0.582	1.40	3.37	4.04	0.117
10	0.483	0.894	2.65	3.04	0.046
14	0.456	0.728	2.41	2.70	0.040
18	0.445	0.646	2.28	2.52	0.037
30	0.433	0.545	2.12	2.28	0.069
50	0.427	0.495	2.03	2.16	0.212

neutrino fluence from i -th GW event assuming isotropic emission is proportional to the radiation mass as follows:

$$\Phi_i = \frac{\epsilon M_{rad_i} c^2}{4\pi R_i^2 \langle E_i \rangle}, \quad (7)$$

where ϵ is a fraction of neutrino radiation and $\langle E_i \rangle$ is the average neutrino energy. The obtained limits on the neutrino fluences can be converted to the limit on the value of ϵ .

According to the GWTC-3 database for 70 BHBH GW events when the Borexino detector was in data tak-

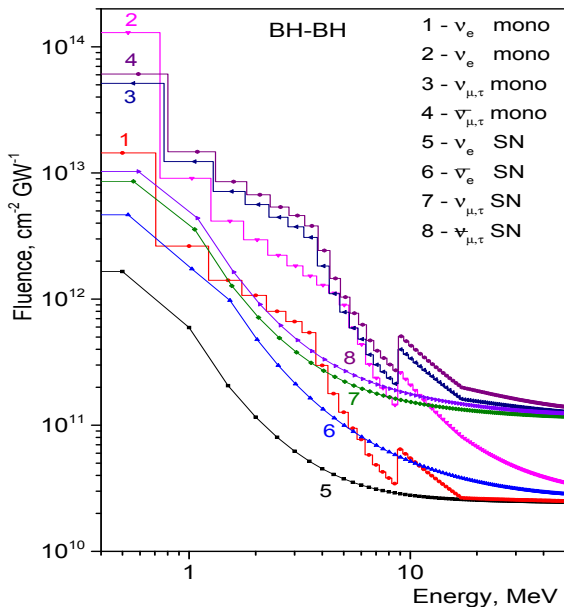


Fig. 7 The upper limits on the neutrino fluences from 26 most intensive HBHB mergers. The mono-energetic neutrinos (Energy= E_ν) - 1- ν_e , 2- $\nu_{\mu,\tau}$, 3- $\bar{\nu}_e$, 4- $\bar{\nu}_{\mu,\tau}$. The neutrinos with SN spectra (Energy= $\langle E \rangle$) - 5- ν_e , 6- $\nu_{\mu,\tau}$, 7- $\bar{\nu}_e$, 8- $\bar{\nu}_{\mu,\tau}$. (all for 90% C.L.).

ing mode, the distances to events R_i lie in the range (0.3 - 8.3 Gpc) and an average distance is $\langle R_i \rangle = 2.1$ Gpc. The corresponding radiative masses M_{rad_i} are inside (0.3 - 9.4) M_\odot interval with average mass $\langle M_{rad_i} \rangle = 2.6 M_\odot$. Therefore, as a reference event, we define the "standard" event with M_{rad} equals one solar mass M_\odot at a distance R_{Gpc} of one Gpc. The upper limits on the neutrino fluence obtained for the single GW event Φ_i can be converted to the limit on the fluence from "standard" GW event as $\Phi_{std} = w_i \Phi_i$ where the weight $w_i = (R_{Gpc}/R_i)^2 (M_{rad_i}/M_\odot)$.

Among 70 BHBH GW events, we selected 26 events, for which weight w_i is greater than 1. For these 26 events, the average distance $\langle R_{26} \rangle$ is 1.0 Gpc, the average radiative mass $\langle M_{rad_{26}} \rangle$ is 2.3 M_\odot , and the factor characterizing the neutrino flux $\langle w_{26} \rangle = 3.1$. Correspondingly, for the remaining 44 events, the average distance is 2.8 Gpc, the radiative mass is 2.9 M_\odot , and the factor $\langle w_{43} \rangle = 0.44$. These 26 most intense events were used to search for an additional contribution to the ± 1000 s temporal interval from the neutrino interactions, the spectrum was represented as mono-energetic neutrinos and neutrinos with a supernova spectrum. Since no statistically significant excesses were found,

the resulting upper limits on the neutrino fluences for all flavors are shown in the Figure 7. Although the upper bounds on the fluences for mono-energetic neutrinos in Figure 7 (line 1-4) turn out to be weaker than in Figure 4, they are obtained for GW events with the expected most intense neutrino fluxes.

8 Limits on the $\bar{\nu}_e$ -fluence from the IBD reaction

As already mentioned, electron antineutrinos can be also detected in the Borexino detector via inverse β -decay (IBD) reaction on protons with energy threshold of $E_{\bar{\nu}_e} = 1.8$ MeV. The cross section of this process is much higher than the one for $(\bar{\nu}_e, e)$ elastic scattering. Additionally, the IBD offers a unique signature given by temporal and spatial coincidence of two correlated events associated with detection of a positron and a neutron. The prompt positron event with visible energy of $E_{\bar{\nu}_e} - 0.784$ MeV accompanied by γ -rays from neutron capture mostly on protons or carbon nuclei with a small probability. As a result, the rate of the events selected as IBD candidates is much lower with respect to the rate of single electron-like events.

The procedure of IBD events selection and the energy spectrum of prompt positron events are described in detail in [39,40,41,43,44]. In the IBD analysis, we used the same E_{up} upper boundary of the visible energy range as in the case of the (ν, e) -scattering analysis. No IBD events were observed in the ± 1000 s interval around the selected GW events and the expected background was almost zero [41,44] that allowed us to use the conservative value of $N_{90}(E_\nu, n_{obs}, n_{bkg}) = 2.44$ in the analysis [59]. Since the cross section of IBD reaction is about two orders of magnitude larger than (ν, e) -scattering cross sections at given neutrino energies, and the background level is smaller, the most stringent upper limits have been obtained for the fluence of electron antineutrinos.

The upper limit on the mono-energetic electron antineutrinos ($\bar{\nu}_e$) fluence using the IBD reaction is calculated from the relation (6) but with reposition of the N_e with the number of protons N_p and considering the cross section of IBD reaction [60]. The resulting limit on $\bar{\nu}_e$ fluence for 74 GW events reduced per one GW event is shown in Figure 8 (line 1) and Tables 3, 4 and 5. For comparison, the limit on $\bar{\nu}_e$ fluence for one GW event (e.g. GW170817 NSNS merge) is presented by line 2 in Figure 8. The limit obtained for all 74 GW events and reduced per single GW is 74 times stronger.

Upper limits on the fluence can be converted into upper limits on the total energy radiated in form of

neutrinos ϵM_{rad_i} for a BHBH, NSNS and NSBH mergers using relation (7). We consider only the energy radiated by 10 MeV electron neutrinos ν_e and antineutrinos $\bar{\nu}_e$ under assumption of isotropic angular distribution of emitted neutrinos. Upper limits on the fluence of ν_e and $\bar{\nu}_e$ from the closest NSNS GW 170817 event obtained for (ν_e, e) -scattering and from IBD reaction (4) lead to restrictions on $\epsilon M_{rad} c^2 \leq 2.9 \times 10^{60}$ erg and $\epsilon M_{rad} c^2 \leq 5.7 \times 10^{58}$ erg, accordingly. These values can be compared with the energy of solar mass $M_\odot c^2 = 1.8 \times 10^{54}$ erg. Accordingly, the restrictions on fraction of neutrino radiation become unnatural and exceed unity ($\epsilon_{\nu_e} \leq 1.0 \times 10^9$ and $\epsilon_{\bar{\nu}_e} \leq 2.0 \times 10^7$). For comparison, we note that if GW170817 event occurred at the same distance as the supernova collapse SN1987A at 51 kpc from Earth, the sensitivity to the energy released in form of 10 MeV neutrinos would be $\epsilon M_{rad} c^2 \leq 8.9 \times 10^{52}$ erg ($0.05 M_\odot$) and $\epsilon_{\bar{\nu}_e} \leq 1.2$.

In the case of 26 most intensive BHBH GW events, the resulting fluence is:

$$\Phi_{tot} = \sum_{i=1}^{26} \frac{\epsilon M_{rad_i} c^2}{4\pi R_i^2 < E_i >}. \quad (8)$$

where the upper limit on the total fluence $\Phi_{tot} = 1.45 \times 10^{12} \text{cm}^{-2}$ (Figure 7) and values M_{rad_i} and R_i can be taken from the GWTC-3 database. Since for 26 GW events the average mass $\langle M_{rad} \rangle = 11 M_\odot$ as well as the average squared distance $\langle R^2 \rangle = 0.5 \text{Gpc}^2$ are about 300 times larger than for the GW 170817 event, the upper limits of the value of $\epsilon_{\nu_e, \bar{\nu}_e}$ are of the same order as for obtained with GW 170917 event.

This suggests that successful detection of low-energy neutrinos should be possible only in case of anisotropic angular distribution of neutrino emission. The limits on energy radiated into neutrinos of other flavors can be easily calculated from Tables 3, 4 and 5.

9 Conclusion

We have searched for signals of neutrino-electron scattering with visible energies above 250 keV within a time window of ± 1000 s centered at the detection moment of a particular GW event. Two types of incoming neutrino spectra were considered: a mono-energetic line and supernova neutrino spectrum given by modified Fermi-Dirac distribution for different effective neutrino temperatures. We searched for coincident neutrino-electron elastic scattering of $\nu_{e, \mu, \tau}$ and $\bar{\nu}_{e, \mu, \tau}$ and IBD of $\bar{\nu}_e$ in the Borexino detector with the 74 GW events associated with the O1, O2 and O3 observing runs of the LIGO/VIRGO detectors. We looked for an excess in the number of Borexino events produced by neutrino-electron elastic scattering and the inverse beta-decay on

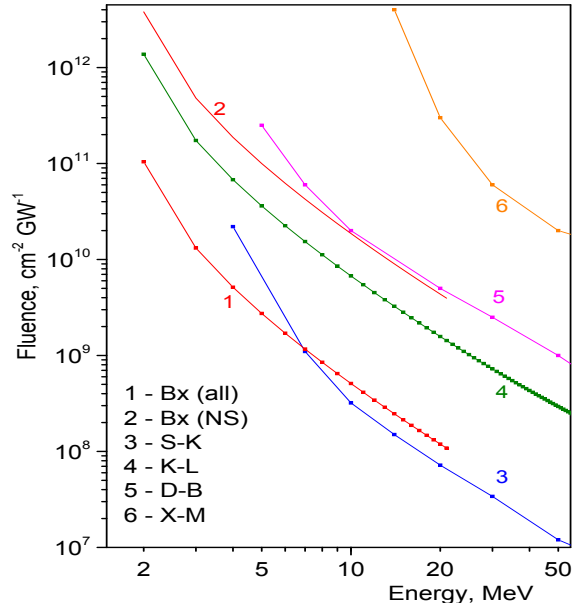


Fig. 8 Upper limits on the fluence of mono-energetic electron antineutrinos $\bar{\nu}_e$ obtained using IBD reaction. 1-Borexino (all 74 GW events, reduced per single GW event), 2-Borexino (GW 170817 NSNS event), 3-Super-Kamiokande coll. [11] (GW 170817), 4-KamLand coll. [16] (GW 170817), 5- DayaBay coll. [13], 6 - XMASS-I coll. [15] (all for 90% C.L.).

protons correlated to 74 GW events from the GWTC-3 database. We found no statistically significant increase in the number of events, with visible energies above 0.25 MeV within time windows of ± 1000 s centered at the moment of GW arrival for all three options for merging of black holes and neutron stars. As a result, new limits on the fluence of monochromatic and supernova neutrinos of all flavors were set for neutrino energies in range of 0.5–5 MeV. Also, the inverse beta-decay reaction was considered in order to set a new limit on the fluence of electron antineutrinos related with the GW events.

Acknowledgements The Borexino program is possible by funding from INFN (Italy), NSF (USA), DFG and HGF (Germany), RSF (Grant 21-12-00063) (Russia), and NCN (Grant No. UMO-2017/26/M/ST2/00915) (Poland). We acknowledge the generous hospitality and support of the Laboratori Nazionale del Gran Sasso (Italy).

References

1. B. P. Abbott et al., (LIGO Scientific Coll. and Virgo Coll.) Observation of Gravitational Waves from a Binary Black

- Hole Merger, *Phys. Rev. Lett.* 116 (2016) 061102
2. B. P. Abbott et al., (LIGO Scientific Coll. and Virgo Coll.) GWTC-1: A Gravitational-Wave Transient Catalog of Compact Binary Mergers Observed by LIGO and Virgo during the First and Second Observing Runs, *Phys. Rev. X* 9 (2019) 031040
 3. B. P. Abbott et al., (LIGO Scientific Coll. and Virgo Coll.) GW170817: Observation of Gravitational Waves from a Binary Neutron Star Inspiral, *Phys. Rev. Lett.* 119 (2017) 161101
 4. GWTC-3: Compact Binary Coalescences Observed by LIGO and Virgo During the Second Part of the Third Observing Run, arXiv:2111.03606v2
 5. S. Adrian-Martinez et al., (ANTARES and IceCube coll.), High-energy neutrino follow-up search of gravitational wave event GW150914 with ANTARES and IceCube, *Phys. Rev. D* 93 (2016) 122010.
 6. A. Aab et al., Ultrahigh-energy neutrino follow-up of gravitational wave events GW150914 and GW151226 with the Pierre Auger Observatory, *Phys. Rev. D* 94 (2016) 122007.
 7. A. Gando et al., (KamLAND coll.) A search for electron antineutrinos associated with gravitational wave events GW150914 AND GW151226 using Kamland, *Astrophys. J.* 829 (2016) L34; A. Gando et al., Erratum: "A Search for Electron Antineutrinos Associated with Gravitational-wave Events GW150914 and GW151226 Using KamLAND" *Astrophys. J.* 851 (2017) L22.
 8. K. Abe et al., (Super-Kamiokande coll.) Search for neutrinos in Super-Kamiokande associated with gravitational wave events GW150914 AND GW151226, *Astrophys. J.* 830 (2016) L11.
 9. M. Agostini et al., (Borexino coll.) A Search for Low-energy Neutrinos Correlated with Gravitational Wave Events GW 150914, GW 151226, and GW 170104 with the Borexino Detector *Astrophys. J.* 850 (2017) 21.
 10. A. Albert et al., Search for High-energy Neutrinos from Binary Neutron Star Merger GW170817 with ANTARES, IceCube, and the Pierre Auger Observatory *Astrophys. J.* 850 (2017) L35.
 11. K. Abe et al., Search for Neutrinos in Super-Kamiokande Associated with the GW170817 Neutron-star Merger, *Astrophys. J.* 857 (2018) L4.
 12. M. A. Acero et al., Search for multimessenger signals in NOvA coincident with LIGO/Virgo detections, *Phys. Rev. D* 101 (2020), 112006.
 13. F.P. An et al., (Daya Bay Coll.) Search for electron-antineutrinos associated with gravitational-wave events GW150914, GW151012, GW151226, GW170104, GW170608, GW170814, and GW170817 at Daya Bay, *Chinese Phys. C* 45, 055001 (2021)
 14. M. A. Acero et al., Extended search for supernovae-like neutrinos in NOvA coincident with LIGO/Virgo detections, *Phys. Rev. D* 104, 063024 (2021)
 15. K. Abe et al., (XMASS-I coll.) Search for event bursts in XMASS-I associated with gravitational-wave events, *Astroparticle Phys.*, 129, (2021), 102568
 16. K. Abe et al., Search for Low-energy Electron Antineutrinos in KamLAND Associated with Gravitational Wave Events, *Astrophysical Journal*, 909:116 (2021), arXiv:2012.12053v1
 17. K. Abe et al., Search for neutrinos in coincidence with gravitational wave events from the LIGO-Virgo O3a Observing Run with the Super-Kamiokande detector, *Astrophys. J.* 918 (2021) 2, 78 arXiv:2104.09196
 18. M. M. Boliev et al., Search for muon neutrinos from the gravitational wave event GW170817 at the Baksan Underground Scintillation Telescope, *J. Phys.: Conf. Ser.* 1787 (2021) 012034
 19. V. B. Petkov et al., Searching for Muon Neutrinos from Regions of the Localization of Gravitational-Wave Events, *Bull. Russ. Acad. Sci. Phys.* 85, 444 (2021).
 20. M. Agostini et al., (Borexino coll.), First Directional Measurement of Sub-MeV Solar Neutrinos with Borexino, *Phys. Rev. Lett.* 128 (2022) 9, 091803
 21. M. Agostini et al., (Borexino coll.), Correlated and integrated directionality for sub-MeV solar neutrinos in Borexino, *Phys. Rev. D* 105 (2022) 5, 052002
 22. G. Alimonti et al., (Borexino Collaboration), Science and technology of Borexino: a real-time detector for low energy solar neutrinos, *Astropart. Phys.* 16, 205 (2002)
 23. G. Alimonti et al., (Borexino Collaboration), The Borexino detector at the Laboratori Nazionali del Gran Sasso. *NIMA* 600, 568 (2009)
 24. H. Back et al., (Borexino Collaboration), Borexino calibrations: Hardware, Methods, and Results, *JINST* 7, P10018 (2012)
 25. G. Bellini et al., (Borexino Collaboration) Final results of Borexino Phase-I on low-energy solar neutrino spectroscopy, 2014 PRD, 89, 112007
 26. M. Agostini et al. (Borexino Collaboration), Simultaneous precision spectroscopy of pp, 7Be, and pep solar neutrinos with Borexino Phase-II *Phys. Rev. D* 100, 082004 (2019).
 27. G. Bellini et al. (Borexino Collaboration), Muon and cosmogenic neutron detection in Borexino, *JINST* 6 P05005 (2011)
 28. C. Arpesella et al. (Borexino Collaboration), Direct Measurement of the 7Be Solar Neutrino Flux with 192 Days of Borexino Data, *Phys. Rev. Lett.* 101, 091302 (2008)
 29. G. Bellini et al. (Borexino Collaboration), Precision Measurement of the 7Be Solar Neutrino Interaction Rate in Borexino, *Phys. Rev. Lett.* 107, 141302 (2011)
 30. G. Bellini et al. (Borexino Collaboration), Measurement of the solar 8B neutrino rate with a liquid scintillator target and 3 MeV energy threshold in the Borexino detector, *Phys. Rev. D* 82, 033006 (2010)
 31. M. Agostini et al. (Borexino Collaboration), Improved measurement of 8B solar neutrinos with 1.5 kt y of Borexino exposure, *Phys. Rev. D* 101, 062001 (2020)
 32. G. Bellini et al. (Borexino Collaboration), First Evidence of pep Solar Neutrinos by Direct Detection in Borexino, *Phys. Rev. Lett.* 108, 051302 (2012)
 33. G. Bellini et al. (Borexino Collaboration), Neutrinos from the primary proton-proton fusion process in the Sun, *Nature* 512, 383 (2014)
 34. M. Agostini et al., (Borexino Collaboration), Comprehensive measurement of pp-chain solar neutrinos, *Nature* 562, 505 (2018)
 35. M. Agostini et al., (Borexino Collaboration), Experimental evidence of neutrinos produced in the CNO fusion cycle in the Sun, *Nature* 587, 577 (2020)
 36. M. Agostini et al., (Borexino Collaboration), Sensitivity to neutrinos from the solar CNO cycle in Borexino, *Eur. Phys. J. C* 80, 1091 (2020)
 37. S. Appel et al., (Borexino Collaboration), Improved Measurement of Solar Neutrinos from the Carbon-Nitrogen-Oxygen Cycle by Borexino and Its Implications for the Standard Solar Model, *Phys. Rev. Lett.*, 129, 252701 (2022)
 38. G. Bellini et al. (Borexino Collaboration), Observation of geo-neutrinos, *Phys. Lett. B* 687, 299 (2010)
 39. G. Bellini et al. (Borexino Collaboration), Measurement of geo-neutrinos from 1353 days of Borexino, *Phys. Lett. B* 722, 295 (2013)
 40. M. Agostini et al., (Borexino Collaboration), Spectroscopy of geoneutrinos from 2056 days of Borexino data, *Phys. Rev. D* 92, 031101(R) (2015)

-
41. M. Agostini et al., (Borexino Collaboration), Comprehensive geoneutrino analysis with Borexino, *Phys. Rev. D* 101, 012009 (2020)
 42. G. Bellini et al. (Borexino Collaboration), Absence of a day–night asymmetry in the ^7Be solar neutrino rate in Borexino, *Physics Letters B* 707, 22 (2012)
 43. G. Bellini et al. (Borexino Collaboration), Study of solar and other unknown anti-neutrino fluxes with Borexino at LNGS, *Physics Letters B* 696, 191 (2011)
 44. M. Agostini et al., (Borexino Collaboration) Search for low-energy neutrinos from astrophysical sources with Borexino, *Astroparticle Physics* 125 (2021) 102509
 45. S.K. Agarwalla et al., (Borexino Collaboration), Constraints on flavor-diagonal non-standard neutrino interactions from Borexino Phase-II The Borexino Collaboration, *J. High Energ. Phys.* 2020, 38 (2020)
 46. G. Bellini et al. (Borexino Collaboration), New experimental limits on the Pauli-forbidden transitions in ^{12}C nuclei obtained with 485 days Borexino data, *Phys. Rev. C* 81, 034317 (2010)
 47. G. Bellini et al. (Borexino Collaboration), Search for solar axions produced in the $p(d,^3\text{He})\alpha$ reaction with Borexino detector, *Phys. Rev. D* 85, 092003 (2012)
 48. M. Agostini et al., (Borexino Collaboration), New limits on heavy sterile neutrino mixing in ^8B decay obtained with the Borexino detector, *Phys. Rev. D* 88, 072010 (2013)
 49. M. Agostini et al., (Borexino Collaboration), A test of electric charge conservation with Borexino, *Phys. Rev. Lett.* 115, 231802 (2015)
 50. M. Agostini et al., (Borexino Collaboration) Borexino’s search for low-energy neutrino and antineutrino signals correlated with gamma-ray bursts, *Astroparticle Physics* 86, 11 (2017)
 51. S. Appel et al., (Borexino Collaboration), Search for low-energy signals from fast radio bursts with the Borexino detector *Eur. Phys. J. C* (2022) 82:278
 52. B. Baret, I. Bartos, B. Bouhou, et al., Bounding the time delay between high-energy neutrinos and gravitational-wave transients from gamma-ray bursts, *Astroparticle Physics*, 35, 1 (2011)
 53. N. Aghanim et al., (Planck collaboration,) Planck 2018 results. VI. Cosmological parameters, arXiv:1807.06209.
 54. I. Esteban, M.C. Gonzalez-Garcia, A. Hernandez-Cabezudo, M. Maltoni and T. Schwetz, Global analysis of three-flavour neutrino oscillations: synergies and tensions in the determination of the mass ordering, *JHEP* 01, 106 (2019), 1811.05487.
 55. I. Tamborra, B. Muller, L. Hudepohl, H.T. Janka and G. Raffelt, High-resolution supernova neutrino spectra represented by a simple fit, *Phys. Rev. D* 86 (2012) 125031 arXiv:1211.3920
 56. C. Lujan-Peschard, G. Pagliaroli and F. Vissani, Spectrum of supernova neutrinos in ultra-pure scintillators, *Journal of Cosmology and Astroparticle Physics*, JCAP 07 (2014) 051
 57. A. Mirizzi, I. Tamborra, H. Janka, N. Saviano, K. Scholberg, R. Bollig, L. Hudepohl, and S. Chakraborty, Supernova neutrinos: Production, oscillations and detection, *Riv. Nuovo Cim.* 39, 1 (2016), arXiv:1508.00785
 58. J.N. Bahcall, M. Kamionkowski, A. Sirlin, Solar neutrinos: Radiative corrections in neutrino-electron scattering experiments, *Phys. Rev. D* 51, 6146, 1995
 59. G.J. Feldman, R.D. Cousins, Unified approach to the classical statistical analysis of small signals, *Phys. Rev. D* 57, 3873 (1998)
 60. A. Strumia, F. Vissani, Precise quasielastic neutrino/nucleon cross section, *Phys. Lett. B* 564, 42 (2003)